Absorption characteristics of a quantum dot array induced intermediate band: Implications for solar cell design

Tomic, S, Jones, T and Harrison, N

http://dx.doi.org/10.1063/1.3058716

Absorption characteristics of a quantum dot array induced intermediate band: Implications for solar cell design

Stanko Tomić,[1,a)] Tim S. Jones,[2] and Nicholas M. Harrison[1,3]
[1]*Department of Computational Science and Engineering, STFC Daresbury Laboratory, Cheshire WA4 4AD, United Kingdom*
[2]*Department of Chemistry, University of Warwick, Coventry CV4 7AL, United Kingdom*
[3]*Department of Chemistry, Imperial College, London SW7 2AZ, United Kingdom*

(Received 27 October 2008; accepted 7 December 2008; published online 29 December 2008)

We present a theoretical study of the electronic and absorption properties of the intermediate band (IB) formed by a three dimensional structure of InAs/GaAs quantum dots (QDs) arranged in a periodic array. Analysis of the electronic and absorption structures suggests that the most promising design for an IB solar cell material, which will exhibit its own quasi-Fermi level, is to employ small QDs (~6–12 nm QD lateral size). The use of larger QDs leads to extension of the absorption spectra into a longer wavelength region but does not provide a separate IB in the forbidden energy gap.
 [DOI: 10.1063/1.3058716]

The power efficiency of a semiconductor single energy gap solar cell (SC) is limited to 41% as the cell voltage cannot be increased without eventually degrading the photocurrent.[1] This can be exceeded by splitting the solar spectrum so that each junction converts a different spectral region. The addition of more junctions ($n>3$) in the SC design, with gradually diminishing efficiency improvements, is limited by increasing complexity and material issues (for instance, the accumulated strain between pseudomorphically mismatched layers).[2] Therefore, significant attention has been paid to developing alternative approaches in which a single SC exceeds the efficiency of a conventional *pn* junction. A promising proposal is the intermediate band SC (IBSC),[3,4] for which, under ideal conditions, an efficiency of 63% can be achieved with a degree of flexibility in the value of the energy gaps and the IB position.[5] The higher efficiency is due to the fact that additional absorption, from valence band (VB) states to the IB and from the IB to the conduction band (CB) states, allows two photons with energies below the energy gap of the barrier material to be harvested in generating one electron-hole pair, in addition to those generated by direct VB-CB transitions. In this way the IBSC overcomes the problem of increasing the SC photocurrent without degrading its voltage. Quantum nanostructures, such as quantum dots (QD), arranged in superlattice (SL) arrays[6–9] can produce a narrow IB within the CB of the QD material and the energy gap of the barrier material. Ideally the IB is separated from the barrier material VB and CB by a region with zero density of states, allowing a quasi-Fermi energy to be maintained under illumination. In this letter we report on the electronic structure and absorption characteristics of a model IBSC material based on a InAs/GaAs QD array and examine their dependence on the QD size and spacing.

The theoretical model of the QD array's electronic structure is based on the eight-band $\mathbf{k}\cdot\mathbf{p}$ Hamiltonian $H(\mathbf{k})$, which includes the k-dependent diagonal and off-diagonal matrix elements, describing mixing between states in the CB and the heavy hole (HH), light hole (LH), and spin-orbit states in the VB, strain, and piezoelectric field. The whole Hamiltonian is derived in the angular momentum basis[10] and is diagonalized exploiting the symmetry of the system.[11] Material parameters of the bulk InAs and GaAs were taken from Ref. 12. The plane-wave (PW) based $\mathbf{k}\cdot\mathbf{p}$ method with periodic boundary conditions is particularly suited for analysis of the QD array structures. The electronic structure of such an array is characterized by a Brillouin zone (BZ) determined by the QD array dimensions. To calculate the electronic structure the only modification to the basis set is to replace the reciprocal lattice vectors in the PW expansion with those shifted due to the QD-SL, i.e., $k_v \rightarrow k_v + K_v^{\mathrm{SL}}$, where $0 \le K_v^{\mathrm{SL}} \le \pi/L_v^{\mathrm{SL}}$ and L_v are the superlattice vectors in the $v=(x,y,z)$ directions. This allows the sampling along the $\mathbf{K}$ points of a QD-SL to be done at several points at the cost of the single QD calculation at each point. The optical matrix element used is defined as $|\hat{e}\cdot\mathbf{p}_{ij}|^2$, where $\hat{e}$ is the light polarization vector and $\mathbf{p}_{ij}(\mathbf{k})=(m_0/\hbar)\langle i|\partial H(\mathbf{k})/\partial\mathbf{k}|j\rangle$ is the electron-hole momentum operator of the quantum structure, where i and j are the initial and final states of the QD-SL. From the $\mathbf{K}^{\mathrm{SL}}$ dependent electronic structure and optical dipole matrix element $\mathbf{p}_{ij}(\mathbf{K})$, the absorption characteristics of the QD array were calculated, in the dipole approximation

$$\alpha(\hbar\omega)=\frac{\pi e^2}{c\epsilon_0 m_0^2 \bar{n}\omega}\sum_{i,j,\mathbf{K}}|\hat{e}\cdot\mathbf{p}_{ij}(\mathbf{K})|^2\delta[E_i(\mathbf{K})-E_j(\mathbf{K})-\hbar\omega], \tag{1}$$

where e is the electron charge, c is the speed of light in vacuum, m_0 is the rest electron mass, $\bar{n}$ is the refractive index of the GaAs, ϵ_0 is the vacuum permittivity, and ω is the light frequency. The delta function $\delta(x)$ is replaced with a Gaussian function $\exp[-(x/\sqrt{2}\Gamma)^2]/(\sqrt{2\pi}\Gamma)$, defined by the phenomenological broadening Γ, to take into account random fluctuations in the structure of the QD array.[12] Finally, the summation is replaced by integration over the wave vector K_z.

The model InAs/GaAs QD array considered here consists of truncated pyramidal QDs with the base length b and truncation factor fixed at $t=0.5$ on top of a 1 ML wetting layer (WL) embedded in the tetragonal-like unit cell Ω of the

a)Electronic mail: stanko.tomic@stfc.ac.uk.

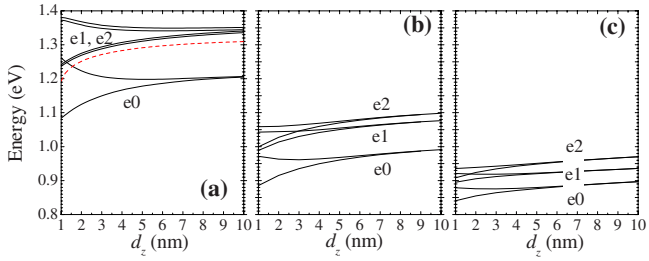

FIG. 1. (Color online) Position of the lower and upper limits of the fundamental (e_0) and excited (e_1,e_2) confined states (measured from the top of GaAs VB) within the CB as they change with the spacer layer distance d_z, for samples (a), (b), and (c) described in the main text. In figure (a) the dashed line is the lower boundary of the WL induced miniband. The position of the WL related miniband is essentially the same in structures (b) and (c) but cannot be distinguished easily from the QD related levels, as can be seen from Figs. 2(b) and 2(c).

size (L_x,L_y,L_z). The vertical periodicity of the QD-SL is controlled by $L_z=d_z+h+L_{\mathrm{WL}}$, where h is the QD height, L_{WL} is the thickness of the WL, and d_z is the variable vertical separation of the QD layers. In the x and y directions the periodicity is kept constant, as d_z is varied, with $L_x=L_y$ chosen to be large enough to prevent lateral electronic coupling. This shape is often found in the QDs under study as can be found from microscopy pictures.[7,8,13]

There are multiple electron and hole states confined within each QD that might form IBs. The variation in the band extrema for the first three IBs as d_z is varied in the range from 1 to 10 nm for three QD sizes [(a) *small* $h=3$ nm, $b=6$ nm, and $L_x=20$ nm; (b) *medium* $h=6$ nm, $b=12$ nm, and $L_x=20$ nm; (c) *big* $h=10$ nm, $b=20$ nm, and $L_x=40$ nm] are displayed in Fig. 1. The band extrema correspond to $K_z=0$ and $K_z=\pi/L_z$, respectively. The width of the IBs, governed by the electronic coupling of QD localized states, is a strong function of d_z. The width of the e_0 IB at the closest spacing $d_z=1$ nm is 177 meV for (a), 86 meV for (b), 38 meV for (c), and almost vanishes by $d_z=10$ nm in all three cases. The trend that e_0, e_1, and e_2 are rising in energy as d_z is increased is attributed to the slow decay of the strain caused by the QDs in surrounding layers.[14] Also, the energy difference between the e_1 and e_2 IB (the two lowest p-like states split due to the piezoelectric field induced C_{2v} symmetry) increases with QD size. This is attributed to the increase in the piezoelectric field with QD size due to an increased QD/barrier material volume ratio in Ω. It is important to note that for the small QD array (a) there is a gap between the e_0 and e_1 IBs of 106 meV at $d_z=4$ nm. Also at this separation the e_0 IB energy width is: 33 meV for (a), 14 meV for (b), and 6 meV for (c). The e_1 and e_2 IBs almost entirely overlap each other in structure (a), while in structures (b) and (c) the small gap appears between e_1 and e_2 for the vertical spacing greater than 3 nm.

For the spacing $d_z=4$ nm the electronic structure of the three QD arrays considered is displayed in Fig. 2 for the $\Gamma\rightarrow X$ path of the QD-SL. As expected, due to the quantum size effect, the optical gap between the electron and hole ground states decreases with increasing QD size. Due to the much higher hole masses, the states in the VB are much more densely spaced. In all three structures considered the states in the VB are spaced much more closely than the thermalization energy at room temperature (25 meV). It is only in sample (a) that energy differences of about 20 meV exist and occur between the topmost five states at the zone boundaries, while in sample (b) differences of ~20 meV occur between h_1 and h_2 states only. At room temperature these bands are therefore essentially continuous. In Fig. 2 the energy of the CB edge at $K_z=0$ is indicated by arrows for all three samples at $(x,y,z)=(0,0,0)$ (the bottom of the QD) and at $(0,0,h)$ (i.e., the QD/barrier interface at the top of the QD). The upper edge defines the energy required for an electron to exit a QD. The different positions of the QD and barrier material band edges, marked by arrows in Fig. 2, on the absolute energy scale occur because of different QD/barrier volume ratios in Ω for the three structures considered. The varying volume ratios produce different conditions for the strain relaxation and piezoelectric fields, which in turn modify differently the band edges throughout the unit cell. With the increasing size of the QDs we also observed a reduced dispersion of the bands and an increase in the electron effective mass.

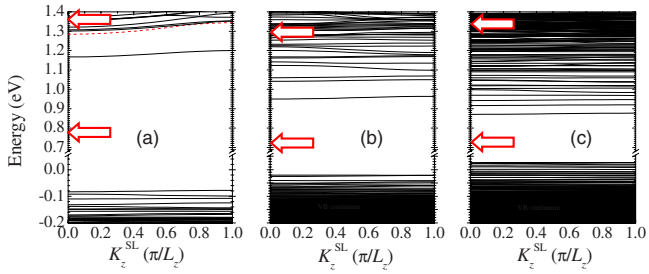

FIG. 2. (Color online) Electronic structure across the $\Gamma\rightarrow X$ path of the first BZ of vertically spaced QD layers of $d_z=4$ nm in all three samples. Horizontal arrows mark the bottom of the CB in QD and top of the CB in the barrier region.

To examine the character and the variation in the optical dipole matrix elements across the IB, in Fig. 3 we display the variation in the $|\hat{e}_x\cdot\mathbf{p}_{e0,j}|^2$ between the electron ground state and the five topmost states in the VB. In structure (a) the ground state hole h_0 is of HH character, and $|\hat{e}_x\cdot\mathbf{p}_{e0,h0}|^2$ is relatively insensitive to K_z. The first exited state in the VB, h_1, is of LH character. Interestingly, at $K_z=0$, the e_0-h_1 transition has a stronger optical dipole element than the e_0-h_0, although there is a rapid decrease as K_z increases. For structure (b) it is clear from the variation in the e_0-LH_1 and e_0-HH_3 optical matrix elements that biaxial strain reduces confinement for the LHs while, at the same time, it increases confinement for the HHs. From Fig. 3(b) it is possible to identify an anticrossing effect between transitions that involve the first and second HH states in the VB, e_0-h_0 and e_0-h_1, respectively, in the vicinity of the $K_z=0.8(\pi/L_z)$. It suggests not only that the complex nature of the biaxial strain in the VB changes the confinement but that it is also

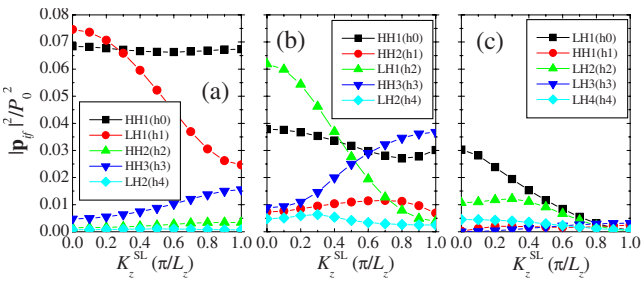

FIG. 3. (Color online) Variation in the optical dipole matrix elements between e_0 and first five states in the VB (h_0-h_4), across the $\Gamma\rightarrow X$ path of the first BZ of vertically spaced QD layers of $d_z=4$ nm in all three samples.

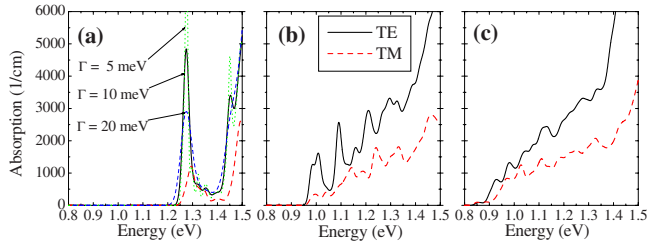

FIG. 4. (Color online) Intraband transversal electric (TE) and transversal magnetic components of the absorption spectra of three representative QD arrays discussed in the main text, calculated with $\Gamma=10$ meV. TE spectra of structure (a) for $\Gamma=5,10,20$ meV (dotted, solid, and dashed lines, respectively) demonstrate the "robustness" of the IB with respect to broadening.

accomplished with a strong HH and LH band mixing that cannot be ignored.[15] For structure (c), in Fig. 3(c), the transition e_0-h_0 involves the hole ground state of the dominant LH character. All dipole matrix elements decrease with increasing K_z. Also, the strength of the e_0-h_0 (LH) at $K_z=0$ is significantly lower than that in the other two structures, suggesting strong delocalization of the LH states. It is apparent that due to the larger QD/barrier material volume ratio in Ω of structure (c) the strain cannot be relaxed in the barrier region, and as it is relaxed in the QD region there is an inversion of the potential for the LHs that delocalize LH states into the barrier material.

Comparison of the absorption characteristics, computed using Eq. (1), of the three representative QD arrays given in Fig. 4 suggests that QD arrays with small to medium QD sizes ($b\sim 6-12$ nm) are the best candidates for the active region of a high efficiency IBSC. Those samples exhibit a well defined absorption peak related to the IB that is separated from the rest of the absorption spectra by a very low density of states, even when line broadening of $\Gamma=10$ meV is assumed. This is essential for providing not only a VB to IB absorption path but also for opening an energy gap between the IB and the rest of CB for a second photon with an energy below barrier material energy gap to be absorbed. Moving from medium to big QDs this peak is reduced and becomes increasingly "hybridized" with the rest of the absorption spectra as the density of both CB and VB states increases due to increased QD size. As a consequence the larger QD array ($b\geq 20$ nm) would behave simply as a bulklike material with a redshifted absorption spectrum extending bulk absorption capabilities toward higher wavelengths, but not providing energy separation for a third quasi-Fermi level within the IB. This statement is valid only if one assumes pure InAs for the QD region. If the amount of In is reduced due to group III intermixing[16] or if In grading within the QD region is assumed,[14] the design of an isolated IB may be possible even with large dots due to an effective reduction in the confinement both in the CB and VB of the QD region, which would facilitate formation of the IBs. The first four optical transitions have recently been observed in photoreflectance measurements, on a QD array structure ($b=10$ nm), for IBSC.[17] Our theoretical results for the similar structure (b) ($b=12$ nm) are in very good agreement, taking into account differences in the QD sizes and the approximations assumed in the model presented here.

Finally we briefly examined the influence of wave function delocalization on the radiative lifetime between e_0 and h_0 ground states. We assume a simplified expression for the radiative recombination lifetime, deduced from the spontaneous emission rate for a bulk material,[18] in which $\tau_{ij}^{\mathrm{rad}} \propto 1/m_r^{*3/2}|\hat{e}\mathbf{p}_{ij}|^2$ and where $m_r^{*-1}=m_e^{*-1}+m_h^{*-1}$ is the reduced effective mass. The results including only the e_0 and h_0 ground states and only calculated at $K_z=0$ are tabulated in Table I. We have estimated that through the introduction of the IB the radiative recombination time can be increased, in most cases, by one order of magnitude over that of a "virtual" bulk GaAs material, which would have the same quasi-Fermi level separation as the particular structure considered here.

TABLE I. Electron, hole, and reduced effective masses, optical dipole matrix element scaled to $P_0=10.3$ eV Å of GaAs bulk, and radiative time scaled to the radiative time of the virtual GaAs bulk with the same quasi-Fermi level separation as in structures considered.

	m_{e0}^*/m_0	m_{h0}^*/m_0	m_r^*/m_0	$\lvert\hat{e}\cdot\mathbf{p}_{ij}\rvert^2/P_0^2$	$\tau_{\mathrm{rad}}/\tau_{\mathrm{rad}}^*$
(a)	0.106	0.553(HH)	0.089	0.061	8.2
(b)	0.118	9.232(HH)	0.117	0.033	10.0
(c)	0.134	0.181(LH)	0.077	0.027	14.2

In summary, the analysis presented here suggests that an appropriately designed QD array will support wave function delocalization and the formation of an IB. As the IB band must be separated from the CB of the host material, a QD array consisting of relatively small (~6–12 nm lateral size) InAs/GaAs dots is the most likely candidate structure for use in the active region of a high efficiency SC. Our analysis suggests that larger QDs in a SL arrangement would simply act to extend the absorption spectra of the GaAs host material toward longer wavelengths.

The authors wish to thank A. Luque and A. Marti for useful discussions. They also wish to thank STFC Energy Strategy Initiative for financial support.

[1] W. Shockley and H. J. Queisser, J. Appl. Phys. **32**, 510 (1961).
[2] M. A. Green, Prog. Photovoltaics **9**, 123 (2001).
[3] A. Luque and A. Marti, Phys. Rev. Lett. **78**, 5014 (1997).
[4] A. Marti, E. Antolin, C. R. Stanley, C. D. Farmer, N. Lopez, P. Diaz, E. Canovas, P. G. Linares, and A. Luque, Phys. Rev. Lett. **97**, 247701 (2006).
[5] S. P. Bremner, M. Y. Levy, and C. B. Honsberg, Appl. Phys. Lett. **92**, 171110 (2008).
[6] Q. Xie, A. Madhukar, P. Chen, and N. P. Kobayashi, Phys. Rev. Lett. **75**, 2542 (1995).
[7] A. Marti, N. Lopez, E. Antolin, E. Canovas, A. Luque, C. R. Stanley, C. D. Farmer, and P. Diaz, Appl. Phys. Lett. **90**, 233510 (2007).
[8] D. Alonso-Alvarez, A. G. Taboada, J. M. Ripalda, B. Alen, Y. Gonzalez, L. Gonzalez, J. M. Garcia, F. Briones, A. Marti, A. Luque, A. M. Sanchez, and S. I. Molina, Appl. Phys. Lett. **93**, 123114 (2008).
[9] R. Oshima, A. Takata, and Y. Okada, Appl. Phys. Lett. **93**, 083111 (2008).
[10] S. Tomić, A. G. Sunderland, and I. J. Bush, J. Mater. Chem. **16**, 1963 (2006).
[11] N. Vukmirović and S. Tomić, J. Appl. Phys. **103**, 103718 (2008).
[12] O. Stier, M. Grundmann, and D. Bimberg, Phys. Rev. B **59**, 5688 (1999).
[13] D. M. Bruls, P. M. Koenraad, H. W. M. Salemink, J. H. Wolter, M. Hopkinson, and M. S. Skolnick, Appl. Phys. Lett. **82**, 3758 (2003).
[14] S. Tomić, P. Howe, N. M. Harrison, and T. S. Jones, J. Appl. Phys. **99**, 093522 (2006).
[15] D. Ahn and S. L. Chuang, IEEE J. Quantum Electron. **24**, 2400 (1988).
[16] P. B. Joyce, T. J. Krzyzewski, G. R. Bell, B. A. Joyce, and T. S. Jones, Phys. Rev. B **58**, R15981 (1998).
[17] E. Canovas, A. Marti, N. Lopez, E. Antolin, P. G. Linares, C. D. Farmer, C. R. Stanley, and A. Luque, Thin Solid Films **516**, 6943 (2008).
[18] S. L. Chuang, *Physics of Optoelectronic Devices* (Wiley, New York, 1995).